REPORT DOCUMENTATION PAGE	*Form Approved* *OMB No. 0704-0188*

The public reporting burden for this collection of information is estimated to average 1 hour per response, including the time for reviewing instructions, searching existing data sources, gathering and maintaining the data needed, and completing and reviewing the collection of information. Send comments regarding this burden estimate or any other aspect of this collection of information, including suggestions for reducing the burden, to Department of Defense, Washington Headquarters Services, Directorate for Information Operations and Reports (0704-0188), 1215 Jefferson Davis Highway, Suite 1204, Arlington, VA 22202-4302. Respondents should be aware that notwithstanding any other provision of law, no person shall be subject to any penalty for failing to comply with a collection of information if it does not display a currently valid OMB control number.
PLEASE DO NOT RETURN YOUR FORM TO THE ABOVE ADDRESS.

1. REPORT DATE *(DD-MM-YYYY)*: 01-07-2005

2. REPORT TYPE: Proceeding

3. DATES COVERED *(From - To)*:

4. TITLE AND SUBTITLE
Morphology of gas bubbles in mud: A microcomputed tomographic evaluation

5a. CONTRACT NUMBER

5b. GRANT NUMBER

5c. PROGRAM ELEMENT NUMBER
N602782N

5d. PROJECT NUMBER

5e. TASK NUMBER

5f. WORK UNIT NUMBER

6. AUTHOR(S)
Allen H. Reed, Bernard P. Boudreau, Chris Algar, Yoko Furukawa

7. PERFORMING ORGANIZATION NAME(S) AND ADDRESS(ES)
Naval Research Laboratory
Seafloor Sciences Branch
Stennis Space Center, MS 39529

8. PERFORMING ORGANIZATION REPORT NUMBER
NRL/PP/7430-05-5

9. SPONSORING/MONITORING AGENCY NAME(S) AND ADDRESS(ES)
Office of Naval Research
800 North Quincy Street
Arlington, VA 22217-5660

10. SPONSOR/MONITOR'S ACRONYM(S)
ONR

11. SPONSOR/MONITOR'S REPORT NUMBER(S)

12. DISTRIBUTION/AVAILABILITY STATEMENT
Approved for public release; distribution is unlimited

13. SUPPLEMENTARY NOTES
Proceedings of the International Conference "Underwater Acoustic Measurements: Technologies & Results" Heraklion, Crete, Greece, 28th June - 1st July 2005.

14. ABSTRACT
Abstract: *Free gas in surficial sediments commonly forms gas bubbles that attenuate and dampen acoustic waves, influence slope stability, and contribute to greenhouse gas concentrations. Therefore, determining the mechanisms that control bubble shape, size, growth, and migration is important to acoustic sediment characterization and other disciplines. Previously, as one component of a sediment acoustic experiment, gas bubble shape, size, and distribution was quantified using "low-resolution" (~500 μm) medical computed tomography (CT). Recently, "high-resolution" (to <25 μm) x-ray micro-computed tomography (XMCT) was used to evaluate gas bubbles in mud; reconstituted in the laboratory, collected near the Mississippi River (MR) mouth, and collected from Cole Harbor*

15. SUBJECT TERMS
computed tomography, methane, gas bubbles, acoustic attenuation, geoacoustics, scattering, damping

16. SECURITY CLASSIFICATION OF: a. REPORT	b. ABSTRACT	c. THIS PAGE	17. LIMITATION OF ABSTRACT	18. NUMBER OF PAGES	19a. NAME OF RESPONSIBLE PERSON
Unclassified	Unclassified	Unclassified	SAR	8	JinWook Kim

19b. TELEPHONE NUMBER *(Include area code)*: 228-688-5473

Proceedings of the International Conference "Underwater Acoustic Measurements: Technologies & Results"
Heraklion, Crete, Greece, 28th June – 1st July 2005

MORPHOLOGY OF GAS BUBBLES IN MUD: A MICROCOMPUTED TOMOGRAPHIC EVALUATION

Allen H. Reed[a], Bernard P. Boudreau[b], Chris Algar[b], and Yoko Furukawa[a]

[a]Marine Geosciences Division, Naval Research Laboratory, SSC, MS, 39529, USA
[b]Department of Oceanography, Dalhousie University, Halifax NS B3H 4J1, Canada

Allen H. Reed, Marine Geosciences Division, Naval Research Laboratory, SSC, MS 39576 USA; FAX: 01 228-688-5473; E-mail: allen.reed@nrlssc.navy.mil

Abstract: *Free gas in surficial sediments commonly forms gas bubbles that attenuate and dampen acoustic waves, influence slope stability, and contribute to greenhouse gas concentrations. Therefore, determining the mechanisms that control bubble shape, size, growth, and migration is important to acoustic sediment characterization and other disciplines. Previously, as one component of a sediment acoustic experiment, gas bubble shape, size, and distribution was quantified using "low-resolution" (~500 μm) medical computed tomography (CT). Recently, "high-resolution" (to <25 μm) x-ray micro-computed tomography (XMCT) was used to evaluate gas bubbles in mud; reconstituted in the laboratory, collected near the Mississippi River (MR) mouth, and collected from Cole Harbor (CH), Nova Scotia. In the reconstituted mud (mixture of kaolinite clay, bay mud, and sucrose), gas bubbles formed spheroids [surface-area ratio (SAR) of ~1.0] with equivalent-bubble radii >30 μm. In several MR cores, gas bubbles formed as vertically oriented oblate spheroids with SARs of ~1.6 (5:1 ratio of length to width), yet in other MR cores, gas bubbles formed elongated fractures that spanned the core width, consequently, a SAR could not be accurately determined. In the CH mud, a gas bubble formed as an oblate spheroid (i.e., coin-shape) with a SAR of ~5.0 (30:1 ratio of length to width) as air was injected incrementally through a capillary tube. It appears that bubble shape (i.e., SAR) and orientation are correlated with sediment physical properties and localized heterogeneity. XMCT images show that gas bubbles grow by fracture mechanics rather than by elastic expansion of the sediments. The images also show that the bubbles exist at sizes that are not resolvable with medical CT, and often grow with the principal axis oriented vertically. XMCT has enabled the characterization of gas bubbles that are significantly smaller than those evaluated previously, thus furthering our mechanistic understanding of gas bubble formation and growth.*

Key words*: computed tomography, methane, gas bubbles, acoustic attenuation, geoacoustics, scattering, damping*

1. INTRODUCTION

1.1. Free Gas: Abundance and Associated Processes

Free gas, such as methane, that is produced during the oxidation of organic matter is ubiquitous in marine sediments [1,2] and when supersaturated produces gas bubbles. Ebullition of methane gas bubbles from sediments is an area of ongoing, highly important research because methane contributes to the greenhouse effect [2] and may initiate mass wasting and landslides [3]. Additionally methane gas bubbles cause acoustic turbidity in regions where gas hydrates occur [4] and greatly elevates acoustic attenuation over that of surrounding non-gaseous sediment [5].

Models of free gas bubble morphology in sediments initiated from images of spheroid bubbles in a fluid. An evolution of thought regarding gas bubble morphology in sediments has developed, because capabilities to x-ray image sediment structures, such as bubbles, has progressed. One capability, computed tomography (CT) has propelled sediment acoustic and geochemical modelling efforts in a new direction; that is, gas bubbles in mud are now modelled as oblate spheroids [6]. The fundamental element lacking from these CT evaluations was the ability to image gas bubbles at high-resolutions and near the point of bubble nucleation [7]. High resolution x-ray microComputed Tomography has substantiated previous evaluations that display/evaluate gas bubble morphology as oblate spheroids, thus elaborating understanding of gas bubble morphology in sediments. Quantification of gas bubbles with orders of magnitude smaller sizes than previously evaluated is possible using x-ray microcomputed tomography (XMCT) images obtained at the Naval Research Laboratory.

1.2. Acoustic Theory of Gas Bubbles

Evaluation of gas bubble morphology in sediments has been driven by the desire to circumvent the enhanced acoustic attenuation that gas bubbles cause; acoustic evaluation of sediments below the gas-laden sediments has been prohibited or impaired. It has been understood for some time that because attenuation in gas-laden mud poses significant challenges to seafloor characterization, there is a need to understand how gas bubble morphology, dynamics and mechanics control determine acoustic propagation and attenuation [5]. Studies to address these issues by direct measurements, using instruments such as the Acoustic Sediment Classification System (ASCS) and CT have provided enhanced understanding of gas bubble morphology and modelling has addressed the influence of this morphology on acoustic behavior [7]. Because attenuation is related to bubble size and shape, accurate determinations of bubble size, shapes, and distributions may enable developments to acoustically image features below the gas-laden sediments [7-9].

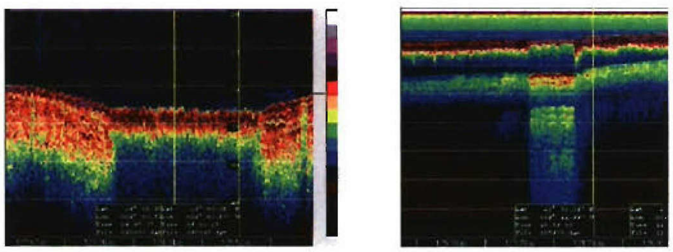

Fig. 1: Image of acoustic impedance data for East Bay (left)(29° 00.85' N, 89°3.53' W) that was collected with ASCS using the ship's 30-kHz transducer. Central region displays high impedance and suggests that free gas is present.

Acoustic attenuation in gas-laden mud occurs as sound is scattered and absorbed. Scattering occurs as the propagated sound is reflected, refracted, and diffracted at the boundaries of the mud and bubble(s); it is proportional to the bubble population. Absorption occurs as acoustic energy is converted to thermal energy during dynamic interactions between gas bubbles and surrounding sediment [5]. Acoustic attenuation is greatest for resonance frequencies (f_0) which for spherical bubbles is related to the bubble radius (r_0) by,

$$f_0 = \frac{1}{2\pi r_0}\left(\frac{3\gamma P_0}{A\rho_w} + \frac{4G}{\rho_s}\right)^{1/2}, \qquad (1)$$

where γ is the ratio of the specific heat of the gas, P_0 is the ambient hydrostatic pressure, A is the gas polytropic coefficient, ρ_w is the density of water, ρ_s is the density of sediment, and G is the sediment dynamic shear modulus [5,7,8]. To determine the shape and size distribution of gas bubbles in a marine mud, a study of Eckernförde Bay was conducted and marine mud was imaged with medical x-ray CT. Bubbles resolved with this system were oblate spheroids and had diameters that ranged from 8.0 to 0.44 mm or the limit of the CT's resolution [8]. Whereas it was noted that numerous bubbles of smaller diameter must exist [7] CT resolution was insufficient to confirm this supposition [6]. However, the finding that gas bubbles in mud were oblate spheroids necessitated a profound divergence in modelling efforts of gas bubble shapes; a surface area ratio (SAR) was used in a sediment bubble scattering model and equation 1 was modified to account for this shape difference. From this effort, model predictions were comparable to the direct measurements on sediment cores, and it was found that oblate spheroids have a lower resonance frequency than spheres with the same volume [8]. The influence of gas volume and bubble size was modelled to determine the correlation between bubble size distributions, reductions in sound speed, and increases in attenuation [9]. Bubbles, which may be modelled with constant dimensions, appear to change size and shape, as determined by changes in resonance frequencies measured during a tidal cycle [10]. Pressure changes during a tidal cycle have also been correlated with bubble migration/ebullition [11]. The relationship between pressure changes, gas bubble morphology and distribution, and changes in sediment properties is complex, requires further exploration, and may necessitate coupling of varied technologies such as CT and impedance tubes, within which pressure and temperature can be controlled.

1.3. IMAGING BUBBLES AND MODELLING BUBBLE GROWTH

Direct evaluations of gas bubble morphology and growth in a viscoelastic media have been reported in several studies and corroborating models have been developed [12-16]. The first in this series was a model, which demonstrated that bubble growth rate is seasonal and controlled by source gas diffusion and it was postulated that the media may control bubble growth [12]. More recently, gas bubbles were grown in a muddy sediment analogue (i.e., gelatin) and natural sediments by the introduction of gas at very precise increments [13]. Mud samples from this study were x-rayed and the images that were produced displayed lineated bubbles, in two dimensions (2D), which were similar to the 2D images produced of bubbles from Eckernförde Bay samples [8]. It was found that bubbles form in gelatin as oblate spheroids with the aspect ratio determined by the cohesive properties of the gelatin [13]. Later it was noted that bubbles grow more quickly by fracture mechanics (i.e., as oblate spheroids) mechanics than by elastic expansion (*i.e.*, as with spheroids) [14, 15]. Additionally, the pressure records indicated that oblate spheroids grow in a succession of

step-wise fractures; as internal gas pressure increases incrementally to a point where resistant forces, or cohesive properties, of the mud are exceeded, whereupon the mud fractures and the bubble grows [14]. Additional evidence that fracture mechanics in elastic media (*i.e.*, gelatin) is a primary mechanism for deformation has been witnessed during polychaete (*i.e.*, *Nereis virens*) burrowing [17]. This fracture phenomenon has also been witnessed in Cole Harbor and East Bay mud where gas bubbles formed as oblate spheroids thus substantiating previous findings in mud and gelatin [16,18].

2. Computed Tomography and Techniques for Evaluation

2.1. Measuring X-ray Attenuation

CT has proven to be a highly valuable tool in the evaluation of heterogeneities within sediments (*e.g.*, shells or gas bubbles) and enables quantification of shapes and sizes of materials that scatter acoustic energy in the seafloor [8,19]. CT non-destructively evaluates sediment cores and enables quantification by measuring attenuation of X-ray energy [19] and differentiates objects that have differences in density and atomic number. Thus, CT provides volumetric images for a variety of sediment samples with varied constituents [20].

The attenuation of x-rays by an object is described by Beer's Law,

$$I_f = I_o \, exp^{(-\mu x)}, \qquad (2)$$

where I_o is incident x-ray intensity, I_f is the x-ray intensity after passing through a sample of diameter x, and μ is the linear attenuation coefficient of the sample. While Beer's Law, in this form, is only applicable to monochromatic energy sources, it may be modified for use with CTs that produce polychromatic energy sources, such as is the case with medical and industrial CTs (*e.g.*, NRL's microfocus x-ray computed tomography [XMCT] system) [20]. During image processing, corrections may be applied to remove artefacts (*i.e.*, beam hardening) associated with nonuniform attenuation within the sample.

2.2. Microcomputed Tomography System at NRL

The XMCT system at NRL is a 3rd generation scanner (Fig. 2); it collects a full swath of the sample material as the sample rotates within the cone-shaped x-ray beam. The x-ray beam has a potential energy of 10-225 keV and 0-3 mA with a resolution potential of <10 μm. To properly image materials with the XMCT, the system and the image intensifier (II) are calibrated for the specific energy and sample material to be evaluated. Once a protocol is established, the sample is placed on a vertical stage, which has 6-fold axis of manipulation, as close to the focal spot as possible. The lead-lined room is sealed, the x-rays are turned on, and the sample is rotated 360° sample between the x-ray source and receiver. Unlike medical CTs, the x-ray source and receiver array are fixed and only the sample material moves. During each rotation of the sample on the vertical stage, image volumes are collected; after one volume of data is collected, the sample is moved vertically, at very precise movements, and a successive image volume is collected. This process is repeated until the entire volume is scanned, which for the 5-cm long cores at 35-μm resolution takes ~seven hours. During each rotation, x-rays are continually emitted and lines of x-ray attenuation data are collected. To achieve desired image quality, the number of lines collected per rotation, the number of times each line is integrated, and the image size is determined (e.g., 256, 512 and 1024).

These combined procedures ensure that the values for each voxel in the image are as finely resolved as possible by generating a large number of attenuation values for each sample. Image files for each data set may be substantial (*e.g.*, ~1 to 4 Gbytes).

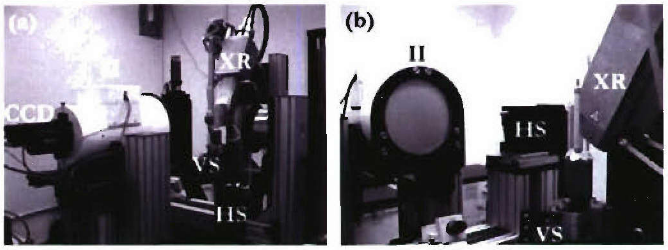

Fig. 2: The XMCT displayed from two views. a) The CT system is comprised, left to right, of a CCD video camera mounted to a Image Intensifier (II), a horizontal stage (HS), the vertical stage (VS) upon which the bubble sample position was manipulated, the sample (S) in a positioning "chuck" and the x-ray tube (XR). b) The CT from the other direction, the x-ray tube (XR) with 2 cooling hoses leading out of the back, the positioning "chuck" with the sample atop the vertical stage (VS), the other side of the horizontal stage (HS) that is opposite of the portion in (a) and the Image Intensifier (II).

Sample resolution is largely determined by how close the item can be placed to the focal spot, which ranges in size from 3 to 8 μm and is automatically determined by source energy. In terms of image resolution for specific sediment sample sizes: for an 8-mm diameter sample, which is placed 15 mm from the focal spot, the maximum sample resolution is ~7 μm; for a 1.5-cm diameter sample, which is placed 30 mm from the focal spot, the maximum image resolution is ~25 μm; and for a 6-cm diameter sample, which is placed 200 mm from the focal spot, the maximum image resolution is ~120 μm. Note that image resolution, or the size of the voxels, is roughly one-half of the material resolution.

The conversion of the x-rays that pass through the sample to photons that the detector can receive is accomplished with a 23cm diameter Image Intensifier (*II*), which converts the x-rays to photons and amplifies the photon signal onto the detector. Pre-scanning calibrations of the *II* are required prior to collecting data, and these are accomplished in the control room (Fig. 3a). Once an image is reconstructed from the raw data, it is displayed on a monitor. During the scanning process, or while the x-rays are turned on, an x-radiograph of the sample material is displayed on a video monitor in the console area (Fig. 3c).

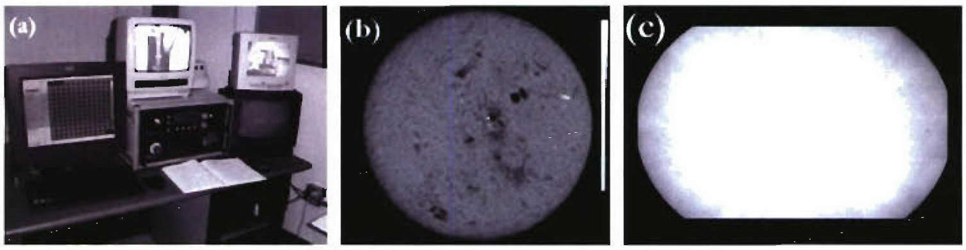

Fig. 3: The control console (a), from left to right, has a monitor [left (a)] for displaying calibrations, position of sample, and reconstructed images (b), the black box [bottom center (a)] controls the x-ray energy, and the monitor [bottom right (a)] provides real-time x-

radiography images (c). Video monitors (a), atop the energy controller and the x-radiography monitor, provide views into the lead-lined CT room.

3. Methods: Preparation of Sediment Samples

Gas bubble morphology was evaluated in sediment samples that were collected from East Bay 29° 00.85' N, 89°3.53' W) and Cole Harbor, Nova Scotia (44° 40.92' N, 63° 32.10' W), and prepared in the lab from a reconstituted kaolinite clay and East Bay mud and in a layer of Ottawa sand. Bubble-rich sediments were located in East Bay with the ASCS and then collected by SCUBA divers, who inserted a 1.5-meter-long, 6-cm diameter, tube into the sediment. The 6-cm diameter tube was predrilled at 5-cm increments with 1.75-cm diameter holes to enable subsamples to be retrieved. The predrilled holes were covered with tape, and upon retrieval of the 1.5-m core to the seafloor surface, divers cut the tape, and inserted 1.5-cm diameter aluminum (Al) tubes through the predrilled holes. During subsampling, compression of the sediments was minimized by retrieving syringes from the Al tubes as the tubes were inserted into the core through the predrilled holes. The 1.5-cm Al tubes were sealed with pressure plugs at the seafloor and recovered to the surface. Cole Harbor Sediments were collected by hand, at low tide, with 6-cm diameter push cores, sealed on both ends, and transported to the lab. Once at the lab, the samples were injected with air pressure using a 'bubble injector device' that is described elsewhere [17]. Reconstituted mud samples were made from a mixture of kaolinite clay that was catalyzed with 1 g of sucrose and inoculated with ~0.4 g of East Bay sediment. The 1.5-cm diameter Al tubes were filled entirely with reconstituted mud or with layers of reconstituted mud and Ottawa sand.

4. Results: Bubbles in Reconstituted and Natural Sediments

Gas bubbles grew in the East Bay and reconstituted muds and a single bubble was injected into the Cole Harbor sediment. In the East Bay mud oblate spheroid bubbles were produced with major axes ranging from 64 μm to 18 mm and minor axes ranging from ~60 to 128 μm, whereas in the reconstituted mud, spherical bubbles were produced with diameters ranging from ~60 μm to 2.5 cm. The gas bubble produced in the Cole Harbor mud had dimensions of 27x20x07 mm^3. Small semi-spherical and disfigured bubbles were present in the sand just above the kaolinite/sand interface. The misshapen forms occur because the bubble wall was compressed against the sand grains. Also, in the kaolinite/sand sample, there were more bubbles in the mud than in the sand. In all cases, these bubbles either filled the interstitial grain space or were bounded by the sediment grains, but never encapsulated the grains.

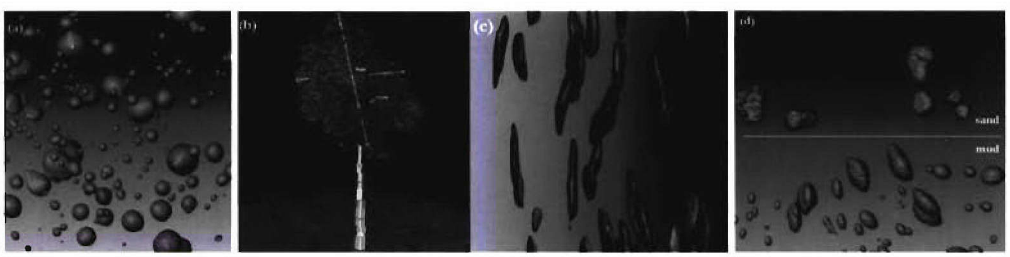

Fig. 5: Bubbles grown in lab and natural mud and in a layered reconstituted mud and sand. Gas bubbles grown in reconstituted kaolinite mud are prolate spheroids and misshapen if

they coalesce (a,d). Gas bubbles grown in Cole Harbor mud (b) and from East Bay mud (c) are oblate spheroids. Prolate spheroids grown in reconstituted mud and sand sections were noticeably misshapen in the sand section with deformation occurring at grain interfaces (d).

5. Discussion and Summary

Understanding gas bubble morphology in sediments and the potential influence upon acoustics has progressed dramatically since the initial evaluations of the effects of gas bubbles on acoustic behavior in an impedance tube [5]. These advances have led to a better understanding of the mechanisms that control acoustic attenuation and sound speed dispersion, the mechanics of gas bubble growth in elastic media, and the forces and processes that enable bubbles to grow and ebulate.

XMCT, used in this study, has demonstrated a) that gas bubbles exist at sizes much smaller than previously determined by CT imagery (~1/10th those previously realized [6]); b) that gas bubbles form differently in reconstituted and natural sediments; c) that in reconstituted mud the probable mechanism for formation is elastic expansion of the sediments, whereas in natural sediments, the probable mechanism for formation is fracture of the sediments; and d) that bubbles probably grow more abundantly in fine-grained sediments, such as mud, than in coarse-grained sediments, such as sand.

This study demonstrates the potential for evaluating relevant processes associated with bubble formation, ebullition, and acoustic attenuation. Because acoustic, geotechnical, and geochemical concerns with respect to bubble morphology and formation are similar, these disciplines can benefit from information about a) the mechanics of bubble formation, b) the controls that sediment properties impose on bubble morphology and population size, c) the potential for bubble growth and migration, and d) the bubble response to changes in temperature, pressure, and other external forces (*e.g.*, sound).

Understanding acoustic attenuation in relation to specific frequencies and gas bubble sizes/distributions is promoted by use of high-resolution systems, such as XMCT, and the ability to image bubbles with different shapes that were either produced or collected (i.e, spheroids, prolate spheroids or oblate spheroids). By coupling x-ray transparent impedance tubes to provide control on the acoustic frequencies with an XMCT that is capable of producing high-resolution images, evaluation of many previously posed questions [see 5-10] may be possible. Questions that can be addressed include: 1) how do bubbles migrate, 2) how do bubble shapes and sizes change as overburden pressure changes, 3) what are the rates of bubble ebullition for spheroids and oblate spheroids, 4) do sediment properties (*e.g.*, stress/strain relationships) change as bubble population increases, and 5) do models accurately predict acoustic attenuation in gas-laden sediments?

6. Acknowledgments

We thank M. D. Richardson for a thoughtful review, E. O. Hartwig for supporting the April 2004 CT workshop, K. B. Briggs and C Vaughan for collecting East Bay samples, B. Johnson for modifying the bubble injection apparatus, H. Eppert for enabling us to obtain software, P. Valent for allowing time to collect this data from the RV Pelican, A. S. Grader and B. Kehl for aid with XMCT, and D. Bibee for use of and aid with the ASCS. This work was supported by the Office of Naval Research, Ocean Acoustics Program and by the Naval Research Laboratory, program element N602782N. Contribution no. NRL/PP/7430-05-5.

REFERENCES

[1] **Fleischer, P., T.H. Orsi, M.D. Richardson, and A.L. Anderson**, Distribution of free gas in marine sediments: a global overview, *Geo-Marine Letters*, vol. 21, pp 103-122, 2001.

[2] **Hovland, M, A.G. Judd, and R.A. Burke Jr**., The global flux of methane from shallow submarine sediments, *Chemosphere,* 26(1-4), 559-578, 1993.

[3] **Hampton, M.A., H. J. Lee, J. Locat**, Submarine landslides, *Rev. Geophys*., vol. 34(1), pp. 33–59, 1996.

[4] **Wood, W.T., J.F. Gettrust, N.R. Chapman, G.D. Spence, and R.D. Hyndman,** Decreased stability of methane hydrates in marine sediments owing to phase-boundary roughness, *Nature,* vol. 420, pp. 656-660, 2002.

[5] **Anderson, A.L. and L.D. Hampton**, Acoustics of gas-bearing sediments I, II. Background, *J. Acoustical Society of America*, vol. 67(6), pp 1865-1903, 1980.

[6] **Abegg, F. and A.L. Anderson,** The acoustic turbid layer in muddy sediments of Eckernförde Bay, Western Baltic: Methane concentration, saturation and bubble characteristics, *Marine Geology*, vol. 137(1-2), pp. 137-147, 1997.

[7] **Richardson, M.D., and A.M. Davis,** Modelling methane rich sediments of Eckernförde Bay, *Continental Shelf Research*, vol. 18(14-15), pp. 1671-1688, 1998.

[8] **Lyons, A.P., M.E. Duncan, A. L. Anderson, and J. A. Hawkins,** Predictions of acoustic scattering response of free-methane bubbles in muddy sediments, *J. Acoustical Society of America*, vol. 99 (1), pp. 163-172, 1996.

[9] **Wood W.T. and M.D. Richardson**; Proceedings, submitted to JASA -frequency and resonance

[10] **Best, A.I., M.D.J. Tuffin, J.K. Dix, and J.M. Bull,** Tidal height and frequency dependence of acoustic velocity and attenuation in shallow gassy marine sediments *J. Geophysical Research-Solid Earth*, vol. 109 (B8), No. B08101, 2004.

[11] **de Angelis, M.A.**, personal communication, 1995.

[12] **Boudreau, B.P., B.S. Gardiner, and B.D. Johnson**, Rate of growth of isolated bubbles in sediments with a diagenetic source of methane, *Limnology and Oceanography*, vol. 46(3), pp. 616-622, 2001.

[13] **Johnson B.D., B.P. Boudreau, and B.S. Gardiner**, Mechanical response of sediments to bubble growth, *Marine Geology*, vol. 187(3-4), pp. 347-363, 2002.

[14] **Gardiner B.S, B.P. Boudreau, and B.D. Johnson**, Slow growth of an isolated disk-shaped bubble of constant eccentricity in the presence of a distributed gas source *Applied Mathematical Modelling,* vol. 27(10), pp. 817-829, 2003.

[15] **Gardiner B.S., B.P. Boudreau, and B.D. Johnson**, Growth of disk-shaped bubbles in sediments, *Geochimica et Cosmochimica Acta*, vol. 67(8), pp. 1485-1494, 2003.

[16] **Boudreau, B.P., I. Croudace, C. Algar, A.H. Reed, B.D. Johnson, K. Dorgan, P.A. Jumars, A.S. Grader, B.S. Gardiner, Y. Furukawa**, Bubble Growth and Rise in Soft Sediments, *Geology*, in press.

[17] **Dorgan, K.M., P.A. Jumars, B.D. Johnson, B.P. Boudreau, and E. Landis**, Burrow extension by crack propagation, *Nature*, vol. 433(7025), pp. 475-475, 2005.

[18] **Algar, C**., unpublished work.

[19] **Wellington, S.L., and H.J. Vinegar**, X-ray computerized tomography, *J. Pertroleum Engineering*, vol. 39(8), pp. 885-897, 1987.

[20] http://www7430.nrlssc.navy.mil/facilities/CTScanner/index.htm